Int. Ed. Engl., 14, 460 (1975).
(11) E. L. Muetterties and L. J. Guggenberger, J. Am. Chem. Soc., 96, 1748 (1974).
(12) W. C. Hamilton in "Structural Chemistry and Molecular Biology", A. Rich and N. Davidson, Ed., W. H. Freeman, San Francisco, Calif., 1968, pp 467–470.
(13) L. C. Thomas, "Interpretation of the Infrared Spectra of Organophosphorus Compounds", Heyden, London, 1974, Chapter 3.
(14) E. Maslowsky, "Vibrational Spectra of Organometallic Compounds", Wiley, New York, N.Y., 1977, pp 109–110.
(15) "International Tables for X-Ray Crystallography", Vol. III, 2nd ed, Kynoch Press, Birmingham, England, 1965.

Coordination Chemistry of Microbial Iron Transport Compounds. 9.[1] Stability Constants for Catechol Models of Enterobactin

Alex Avdeef, Stephen R. Sofen, Thomas L. Bregante, and Kenneth N. Raymond*

Contribution from the Department of Chemistry and Materials and Molecular Research Division, Lawrence Berkeley Laboratory, University of California, Berkeley, California 94720. *Received October 26, 1977*

Abstract: The stability constants of ferric complexes with several substituted catechol (1,2-dihydroxybenzene) ligands in aqueous solutions of low ionic strength have been determined at 27 °C in the pH range 2–11. These simple compounds are used as models of the catechol-containing iron transport compounds (siderophores) found in microorganisms. Enterobactin, the principal siderophore of enteric bacteria, is a tricatechol and, from the formation constants reported here, is estimated to have a formation constant with ferric ion which is greater than 10^{45}. The stepwise formation constants, K_n, of the catechol ligands reported here are defined as $[ML_n]/[ML_{n-1}][L]$, in units of L mol^{-1}, where [L] is the concentration of the deprotonated catechol ligand. The constants were determined from potentiometric and spectroscopic data and were refined on pH values by weighted least squares. Qualitative examination of electron spin resonance spectra of some of the systems indicated some oxidation of the ligand by ferric ions at pH values as high as 4. The ligands studied included catechol (cat) (log K_1 = 20.01, log K_2 = 14.69, log K_3 = 9.01); 4,5-dihydroxy-*m*-benzenedisulfonate (Tiron) (log K_2 = 15.12, log K_3 = 10.10); 4-nitrocatechol (ncat) (log K_1 = 17.08, log K_2 = 13.43, log K_3 = 9.51); 3,4-dihydroxyphenylacetic acid (dhpa) (log K_1 = 20.1, log K_2 = 14.9, log K_3 = 9.0); and 2,3-dihydroxybenzoic acid (dhba) (log K_1 ≈ 20.5). The acid dissociation constants, K_as, were determined also. For the catechol protons these follow: cat (pK_{a_1} = 9.22, pK_{a_2} = 13.0); Tiron (pK_{a_1} = 7.70, pK_{a_2} = 12.63); ncat (pK_{a_1} = 6.65, pK_{a_2} = 10.80); dhpa (pK_{a_1} = 9.49, pK_{a_2} = 13.7); and dhba (pK_{a_1} = 10.06, pK_{a_2} = 13.1). In addition, carboxylate substituents of dhpa and dhba have pK_as of 4.17 and 2.70, respectively. In acidic solution there is evidence of coordination by dhpa via the carboxylate group (which presumably does not involve chelation). Similar coordination by dhba does involve chelation (the same as salicylate) and the system is complicated by mixed-mode coordination of both catechol and salicylate type. In solution, exchange is slow between these two types of coordination following changes in pH.

Introduction

The siderophores (previously called siderochromes)[2] are a class of low molecular weight chelating agents which are manufactured by microorganisms, in response to an iron deficiency, and which facilitate uptake of iron into the organisms. The profound insolubility of ferric hydroxide and the low equilibrium concentrations of ferric ion in biological environments are overcome by the enormous stability and ion selectivity of the ferric siderophore complexes. One important siderophore is enterobactin[3] (Figure 1), the iron sequestering agent for enteric bacteria such as *Escherichia coli*. Since iron is an essential nutrient for all pathogenic bacteria and since the availability of iron often limits the rate of bacterial growth, the siderophores have considerable medical importance.[2] Of particular interest are the formation constants of the ferric siderophore complexes, since these constants define the limits for conditions in which iron will be extracted from other biological ferric complexes in the host organism.

The chelating moieties in enterobactin are catechol (1,2-dihydroxybenzene) groups. Catechol-containing molecules are of widespread biological occurrence and importance. A major class are the catecholamines, which function as neurotransmitters[4] and are of pharmacological use in such diverse areas as the treatment of Parkinson's disease,[5] hypertension,[6] and breast cancer.[7] It has been proposed that the antihistamine action of some of these catechols is related to competition with histamine for the receptor sites, which may be metal ions.[8] Ferric ions can inhibit the constrictor response of adrenaline, an effect attributed to the oxidation of the catechol by the metal.[9] Vanadium catechol complexes have been reported to have nitrogen fixation activity.[10]

It has been recognized for some time that ferric ions can form very stable complexes with catechol ligands.[11] For example, adrenaline can extract iron from ferritin.[9] Although there have been several studies of the stabilities of ferric complexes with catechol-containing ligands,[12-20] no general correlation of the stability of these complexes with electronic and steric substituent effects of the ligands has been found. In acidic aqueous solutions (pH 1–2), Mentasti and co-workers[19,20] studied the formation of 1:1 (metal to ligand) ferric complexes with a wide variety of catechols using stopped-flow and spectroscopic techniques.

Our interest in the coordination chemistry of enterobactin has led to the study of simpler catechol complexes as models for the more complicated biological molecules.[21] The extensive hydrolysis of enterobactin in even mildly basic solutions (pH >8), involving the cleavage of the ester linkages, precludes the direct determination of its proton dissociation constants. Moreover, its ferric complex appears to be oxidatively unstable in acidic medium. It was thus important to establish, by the use of readily available simple compounds, (1) a realistic lower bound for the formation constant of ferric enterobactin and related biological compounds, (2) the extent and nature of the

0002-7863/78/1500-5362$01.00/0

oxidative instability, and (3) the effect of the substituent groups on the complex stability.

The present study extends and reexamines previous determinations of stability constants of ferric–catechol complexes to a wider range in hydrogen ion concentration (pH 2–11), using both potentiometric and spectroscopic techniques. The ligands chosen for the study exhibit a considerable range in proton dissociation constants and include catechol (cat, **1**), 4,5-dihydroxy-*m*-benzenedisulfonate (Tiron, **2**), 4-nitrocatechol (ncat, **3**), 3,4-dihydroxyphenylacetic acid (dhpa, **4**), and 2,3-dihydroxybenzoic acid (dhba, **5**). Ferric complexes with

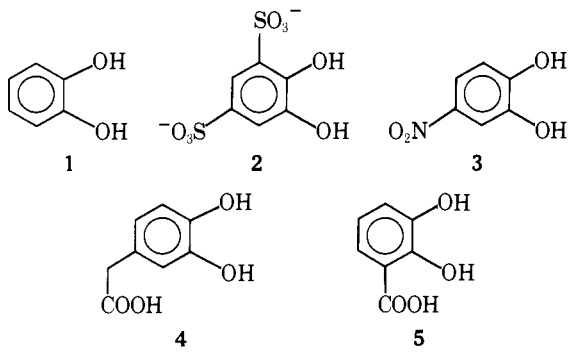

Tiron (**2**) have been studied extensively with the aim of finding analytical reagents for the metal ion.[12,13] Complexes with dhba (**5**) in ethanol–water solutions[14] have also been examined using spectroscopic techniques.

Experimental Section

Since catechol molecules are rapidly oxidized by molecular oxygen in basic solutions, all solutions were kept under an oxygen-free argon atmosphere in a glove box which incorporates a recirculating gas purification system.

Microanalyses were performed by the Microanalytical Laboratory, Department of Chemistry, University of California, Berkeley.

Distilled and deionized water was redistilled in an all-glass apparatus and stored in the glove box.

Reagents and Other Chemicals. Ferric stock solutions (~0.1 M in 0.1 M HCl) were prepared from ferric chloride hexahydrate (Mallinckrodt, analytical grade) and standarized both spectrophotometrically[22] and by ignition of samples of the solution to constant weight in the oxide Fe_2O_3 (900 °C, 12 h).[23]

Catechol (a generous gift of Crown Zellerbach), dihydroxyphenylacetic acid (Calbiochem, A grade), and dihydroxybenzoic acid (Aldrich Chemical Co.) were used as received since Gran plots[24] of the ligand potentiometric data indicated high purity (100.0, 99.5–99.8, and 99.8%, respectively).

Tiron monohydrate (Eastman Organic Chemicals, erroneously labeled as the anhydrous material) was recrystallized by slow evaporation of a concentrated aqueous solution in a partially evacuated desiccator containing P_2O_5.

Anal. Calcd for $C_6H_4O_8S_2Na_2 \cdot H_2O$: C, 21.69; H, 1.82. Found: C, 22.01; H, 1.89.

Nitrocatechol (Aldrich Chemical Co., 97%) was similarly recrystallized. The large, chunky, yellow crystals were ground and thoroughly dried.

Anal. Calcd for $C_6H_5O_4N$: C, 46.46; H, 3.25; N, 9.03. Found: C, 46.69; H, 3.27; N, 8.89.

Phthalate, phosphate, and borax primary standard buffer solutions[25] were prepared from highly purified potassium hydrogen phthalate, $HKC_8H_4O_4$ (National Bureau of Standards, acidimetric standard), potassium phosphate, KH_2PO_4 (Mallinckrodt, analytical grade, dried at 130 °C prior to use), sodium phosphate, $Na_2HPO_4 \cdot 7H_2O$ (Mallinckrodt, analytical grade, dried at 130 °C to constant weight and stored in a desiccator over P_2O_5 prior to use), and sodium tetraborate, $Na_2B_4O_7 \cdot 10H_2O$ (Sigma Chemical Co., 99.9%).

The 1 M HCl titrant solution was prepared by diluting an "analytical concentrate" (J. T. Baker Chemical Co.) and was standardized with ground and dried[26] tris(hydroxymethyl)aminomethane ("Trisma Base", Sigma Chemical Co.). The 1 M KOH titration solution, carbon dioxide free, was purchased from Orion Chemical Co. and standarized with potassium hydrogen phthalate. A Gran plot[24] confirmed the absence of carbonate. The standardization of titrant solutions were repeated at least four times (standard deviations typically 0.2%).

ENTEROBACTIN

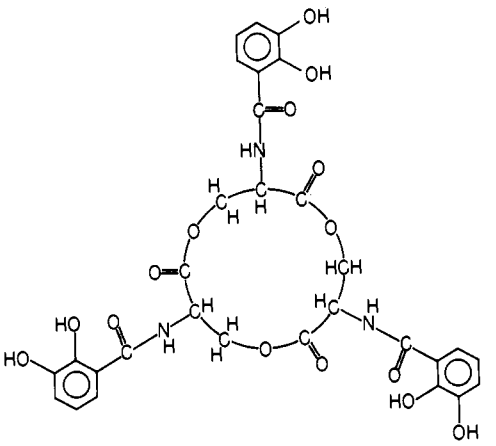

Figure 1. Structural diagram of enterobactin, the siderophore for enteric bacteria.

Potentiometric Titrations. The potentiometric investigations were carried out in beakers suspended in a water-jacketed cell maintained at 27.0 ± 0.1 °C by means of an external constant-temperature circulation bath. (This was expedient since the ambient temperature in the glove box was 23–28 °C.) A digital Corning Model 112 pH meter (equipped with an automatic temperature compensation probe) was used. The combination electrodes [Metrohm (type AE120-2105), Sargent-Welch Miniature (S-30070-10), and Corning semimicro (no. 476050)] were calibrated using the two standard buffer solutions nearest the pH range of interest. Volumes of solutions were dispensed with calibrated volumetric flasks or class A pipets. Titrant or small volumes were delivered with an ultraprecise Gilmont digital micrometer buret (glass plunger, 2.5 mL maximum volume). Supporting electrolyte was not added to the solutions in the study (vide infra).

Readings of pH were taken with the stirring motor off. In cases where there were systematic drifts in the pH, equilibrium was arbitrarily defined to be reached when the drift was less than 10^{-3} pH min^{-1}. Most of the iron catechol complexes studied showed such drift in certain pH ranges and on some occasions it was necessary to wait as long as 1 h for each point. A higher ligand to metal ratio reduced this time. Similar behavior in related compounds has been observed in the past.[15,27] For pH < 4, such drift was not observed and the data were collected faster in order to minimize oxidation of the ligands by ferric ion.

Spectroscopic Measurements. Visible absorption spectra were measured using Cary Model 17 and Model 118 UV–vis spectrophotometers. Typically a basic solution of the metal complex (approximately 1 mM in metal and sixfold excess in ligand) was prepared in the glove box and dispensed in equal portions to several jars equipped with lids. Varying amounts of acid titrant were added. Spectra and pH readings were taken then and several days later, using tightly stoppered cylindrical quartz cells with 0.1-cm path length.

For electron spin resonance (ESR) measurements the solutions were prepared in a similar manner; however, immediately after the desired amount of acid was added, aliquots were withdrawn and transferred to quartz ESR tubes. The tubes were capped with a rubber septum, removed from the glove box, quickly frozen in liquid nitrogen, and sealed with a torch. The ESR spectra were recorded at −196 °C on a Varian E-3 spectrometer at 9.115 GHz.

Computational Methods

Potentiometric. A computer program, STBLTY,[28] was written for the computation and refinement of the formation constants. Although similar in some respects to the programs SCOGS[29] and MINIQUAD,[30,31] STBLTY has several unique features. General multireactant systems (including mixed ligand, polynuclear, and hydrolysis species) can be treated and

any potentiometric data, including pH points, can be utilized. The function minimized is the sum of the weighted[32] squared differences between the observed and calculated dependent variables, such as values of pH (and pM or pL if these are entered as observables[33]). The parameters can be either the logarithm of the overall stability constants (β's) *or* the logarithm of the stepwise formation constants (K's).[34,35] For each point the observed dependent variables and the equilibrium constants are used to calculate, iteratively, the logarithm of the unobserved free reactant concentrations using the mass balance constraints imposed by the stoichiometries of the various equilibrium reactions.[31] Unlike MINIQUAD, STBLTY does not treat the unknown free concentrations as parameters in the same sense as the stability constants. The initial and successive guesses for the unknown concentrations are obtained with a highly successful extended-bootstrap procedure, as described by Maggiore et al.[36] in which

$$pX_{n+1} = pX_n - 0.85\,(pX_{n-1} - pX_n) \times (pH_n - pH_{n+1})/(pH_{n-1} - pH_n)$$

where pX = −log [X], X = M or L. After the unknown dependent variables are determined, the procedure is in turn applied to calculating the observed dependent variables, for the same data point. The weighted differences arising at this stage are those used in the end of normal matrix buildup to determine the best set of parameters. More explicit details of this procedure will be presented in a future publication.[28]

Since no attempt was made to control the exact strength of the ionic medium (it was our desire to work with low ionic strength media), it was necessary to make slight corrections to the stability constants owing to changes in the ionic strength. Therefore the ionic strength is calculated at each point. Since the value of the ionic strength depends on the calculated concentrations, and they in turn (to a lesser extent) depend on it, the procedure is repeated iteratively to self-consistency. For each data point the stability constants are modified from a designated base value of the ionic strength μ_0 (typically 0.1 M) by the expression

$$\log \beta(\mu) = \log \beta(\mu_0) + \Delta z^2 (U(\mu) - U(\mu_0))$$

where Δz^2 is the sum of the squared charges of the reactants minus the squared charge of the associated complex, and

$$U(\mu) = -A\left(\frac{\mu^{1/2}}{1 + \mu^{1/2}} - 0.3\,\mu\right)$$

where A is the usual Debye–Hückel constant (0.5115 at 25 °C).[37]

Typically such corrections amount to less than a third of a log unit since our media usually ranged from 0.05 to 0.25 M in ionic strength. Since the correction implicitly depends on *differences* in activities rather than on absolute values, as a function of changing ionic strength, the theoretical model compares surprisingly well (±3%) with experimentally observed changes in stability constants for $\mu < 0.5$ M.[13] Since the activities of highly charged ions are highly complex quantities, this agreement may be fortuitous.

The stability constants (at ionic strength μ_0) are refined by numerical Gauss–Newton least squares. As in MINIQUAD, the calculated shifts are linearly optimized in the early state of refinement to minimize overshifting problems associated with nonlinearity of the normal equations in regions where poor initial guesses for the parameters have been made.

Crude estimates of the formation constants were obtained from a Bjerrum plot[38] of $\bar{n}$, the average number of coordinated ligands, vs. pL. Similarly, the ligand proton association constants were obtained from a formation curve of $\bar{h}$, the average number of protons attached to the ligand, vs. pH. These secondary concentration variables were derived from experimental data as[39]

$$\bar{n} = \left[C_L - \left(C_H - \frac{a_H}{\gamma_{HCl}} + \frac{K_w}{a_H \gamma_{KOH}}\right)\Big/ \bar{h}\right]\Big/ C_M$$

$$[L] = \left(C_L - \bar{n} C_M\right)\Big/ \sum_{j=0}^{N_h} \beta_j^H [H]^j$$

with

$$\bar{h} = \sum j\beta_j^H [H]^j / \sum \beta_j^H [H]^j$$

and

$$\beta_0 \equiv 1$$

where C_L, C_M, and C_H are the (total) analytical concentrations of the ligand (which contains N_h dissociable hydrogens), metal, and hydrogen, respectively; β_j^H's are the cumulative proton–ligand association constants;[35] and a_H is the activity of the hydrogen ion. In the case of ligand-only data (no metal ion present) the experimental activity coefficients[23] γ_{HCl} and γ_{KOH} (dependent on ionic strength) are used to convert a_H to $[H^+]$ or $[OH^-]$.

$$\bar{h} = \left(C_H - \frac{a_H}{\gamma_{HCl}} + \frac{K_w}{a_H \gamma_{KOH}}\right)\Big/ C_L$$

A succinct three-digit notation which describes each metal–ligand species in solution will be used throughout this paper. For the reaction

$$mM + lL + hH^+ \rightleftharpoons M_m L_l H_h$$

the species $M_m L_l H_h$ is designated by the indexes mlh, in that order. Reactions involving hydroxide are considered as evolving H^+ and so h is negative and is written $\bar{h}$. Thus the species 120 contains one metal ion, two fully deprotonated ligands, and no associated protons, while the species 21$\bar{2}$ contains two metal ions, one ligand, and two hydroxides (or doubly deprotonated ligand).

Weighting Scheme. The weighting scheme used takes into account that the values of pX (X = H, M, L: observed dependent variables) will be least certain (and least important as far as the refinement of the stability constants is concerned) in regions where the slope of the titration curves is the largest (at equivalence points, for example). Thus

$$\sigma^2(pX) = \sigma_I^2 + \left(\frac{dpX}{dV}\right)^2 \sigma_V^2 = (\text{weight})^{-1}$$

where σ_I is a constant term dependent on the electrode and pH meter characteristics and σ_V is the uncertainty in the volume of the titrant added. In our studies, typically σ_I = 0.001–0.005 pH and σ_V = 0.0002–0.002 mL, using the assumption that only random errors are present and thus the goodness of fit[40] should be unity.

In terms of error analysis, STBLTY introduces the use of normal probability plots of the Abraham–Keve type[41] to the assessment of equilibrium models using potentiometric data. This involves a comparison of the ordered distribution of experimental errors, $(pX^{obsd} - pX^{calcd})/\sigma(pX)$, to that expected from a normal (Gaussian) distribution of the same sample size.[42a] An added feature includes the estimation of errors in the species distribution curves as a function of pX, by using error propagation theory (the source of the error bars in Figure 6).

Spectroscopic. The Vareille method[12c] as described by McBryde[13] was used to determine some of the formation constants for the ferric complexes of **1** and **5.** This technique applies to cases where the absorption spectra of the various species present in solution are sufficiently different and where no more than two species are present at any particular pH. When these conditions are satisfied, plots of spectra as a function of pH will show isosbestic points corresponding to

Table I. Ligand Acid Dissociation Constants[a]

	ligand				
	cat	Tiron	ncat[c]	dhpa	dhba
C_L, mM	38.1	50.1	36.6	50.0	21.0
pH range	7.7-12.5	6.5-11.9	5.0-11.0	3.1-12.7	2.3-12.0
μ range, M	0.02-0.10	0.16-0.36	0.02-0.08	0.10-0.32	0.02-0.08
catechol pK_{a_1}	9.22 (3)	7.70 (1)	6.65 (1)	9.49 (3)	10.06 (2)
catechol pK_{a_2}	13.00 (7)[d]	12.63 (5)	10.80 (2)	13.7 (5)	13.1 (2)
substituent pK_a				4.17 (6)	2.70 (3)
no. of data	104	116	101	163	84
GOF[b]	2.7	1.0	1.3	7.3	2.3
(σ_I, σ_V)[e]	(0.6, 1.0)	(1.0, 1.0)	(0.5, 0.2)	(1.0, 0.1)	(0.8, 0.1)

[a] Except as noted, constants were determined at 27.1 °C. [b] Goodness of fit. See text. [c] 28.7 °C. [d] The number in parentheses here and elsewhere in the text refers to the estimated standard deviation in the least significant digit in the corresponding parameter. These are the esd's for the accuracy of the constants as derived from the precision esd's given by least-squares minimization (see text). [e] The units of σ_I are pH × 10^3; those of σ_V are μL.

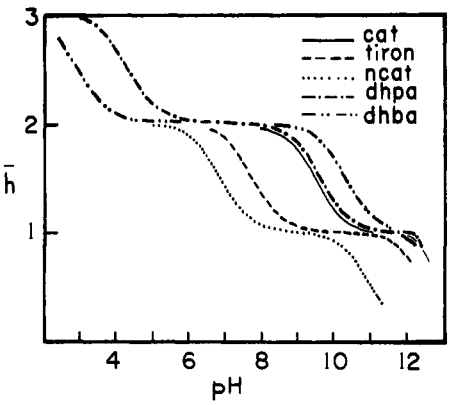

Figure 3. Experimental ligand deprotonation curves, no metal ions present. The parameter $\bar{h}$ is the number of hydrogen ions bound per ligand molecule.

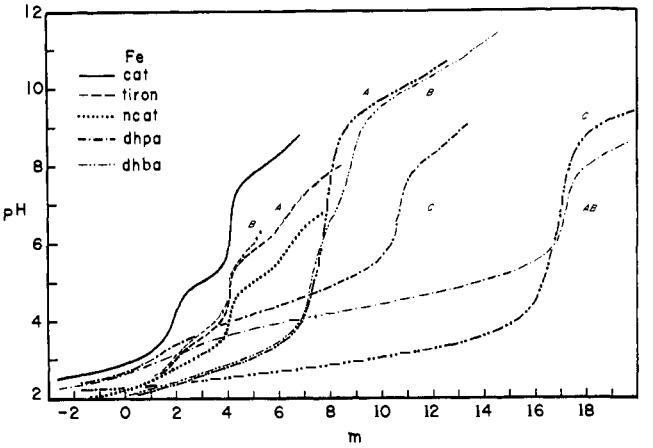

Figure 4. Metal-ligand titration curves. Here, $m = (C_B - C_A)/C_M$, where C_B and C_A are the concentrations of the mineral base (titrant) and acid added initially, respectively, and C_M is the analytical metal concentration.

interconversions between species. By identifying the individual absorption coefficients one can calculate the equilibrium constants associated with equilibria such as

$$ML_{n-1} + H_mL \rightleftharpoons ML_n + mH$$

Results

Potentiometric Data. Tables I and II summarize (and Figures 2 and 4 depict)[42b] the results of the titration study. All the constants listed refer to ionic strength of 0.1 M (vide supra).

Ligand Titrations. The uncontrolled ionic strength varied the most in titrations of the ligand with no metal present, but was generally near 0.15 M.

In the case of the metal-ligand titrations, the ionic strength remained fairly constant over the pH range studied. The dhpa value for pK_{a_2} is suspect owing to the asymmetry about $\bar{h}$ = 1 (Figure 3) in the formation curve. The larger value of the corresponding esd reflects this. The exact reason for this anomaly is not clear, but is probably related to the use of glass electrodes (calibrated only with NBS buffer solutions) in the high pH region. With the above exception, the ligand formation curves, shown in Figure 3, are generally symmetric, as expected.

Ferric-Catechol and -Nitrocatechol. Ferric-catechol and -nitrocatechol systems, in the pH ranges studied, were the only cases successfully fitted with a simple binary metal-ligand model. Below pH 2.3, ferric catechol solutions quickly discolored and an iron-free brown residue precipitated. Over short periods of time this apparently is a reversible process, since the addition of base quickly dissolved the solid and the dark red color of the tris complex reappeared, although slowly. None of the other systems studied gave a precipitate in acidic solutions, although the blue solution of Fe-dhba and the green solution of Fe-dhpa discolored slowly to light yellow and orange, respectively. Prolonged exposure of the latter solutions to oxygen did not appear to produce further discoloration.

Ferric-Tiron. Surprisingly, the Tiron data below pH 2.5 for both concentrations studied failed to show $\bar{n} < 1$. It was thus not possible to refine (nor deduce) $\log K_1$. Possible reasons for this may be: (a) the ligand is being oxidized by the metal, releasing protons in the process, thus increasing $\bar{n}$; (b) the dissociation rate of the 1:1 complex was much slower than allowed for in the experiment; or (c) the electrode was malfunctioning. It seems that (b) is the most likely explanation, since Tiron has the highest reduction potential[20] of the catechols studied and the integrity of the glass electrode was generally above suspicion for pH >2.

The distribution curves for Fe-cat, Fe-Tiron, and Fe-ncat (not shown) are simpler than those for dhpa or dhba (following discussion), and indicate the presence of simply mono, bis, and tris complexes in the pH ranges (3.3-4.5, 6.0-7.0, >8.5), (<2,8, 4.1-5.2, >6.8), and (1.8-2.4, 3.5-4.2, >5.4), respectively, for $C/C_M > 0.9$.

Ferric-Dihydroxyphenylacetic Acid. The Fe-dhpa formation curves (Figure 5b) for the two concentration ratios studied show excellent overlap in the region of $\bar{n}$ 0.6 to 3.0, indicating the absence of polynuclear complexes (such as those possible with such a bifunctional ligand[45]). The absence of a discrete plateau for $\bar{n}$ = 1 suggests that, in acidic solutions, the acetate

Table II. Stability Constants for Ferric Ion with Substituted Catechols

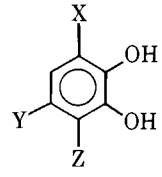

i

	catechol										
	cat. **1**,	Tiron, **2**		ncat, **3**		dhpa, **4**		dhba, **5**			
	1[l]	2A[l]	2B[l]	3[l]	4A[l]	4B[l]	4C[l]	5A[l]	5B[l]	5C[l]	av values
X[a]	H	SO_3^{2-}		H		H			H		
Y[a]	H	SO_3^{2-}		NO_2		CH_2CO_2H			H		
Z[a]	H	H		H		H			CO_2H		
C_M, mM	0.98	4.41	4.00	4.22	1.57	1.57	3.01	4.27	4.09	1.54	
C_L/C_M	6.0	6.5	2.8	6.3	13.3	13.3	6.7	5.3	5.9	14.5	
pH range	2.5-8.8	2.4-7.0	2.5-6.3	1.4-6.8	2.3-8.6	2.3-8.6	2.3-9.0	2.3-10.7	2.3-10.8	2.2-10.5	
μ range, M	0.08	0.10-0.26	0.15-0.25	0.09-0.15	0.06-0.08	0.06-0.08	0.05-0.07	0.11-0.15	0.07-0.13	0.09-0.13	
log K_1*[k]	−2.21 (8)[c]	−0.27[d]	−0.27	−0.37	−3.7 (3)	−2.9 (4)	−3.1 (2)	−1.7 (3)	−4.6 (4)	−1.9 (9)	
				(10)		−8.3 (1)	−8.3 (1)	−16.1 (1)	−14.5 (4)	−15.6 (2)	
log K_2*	−7.53 (2)	−5.45 (10)	−5.22 (6)	−4.02 (4)	−8.3 (1)	−14.4 (1)	−14.2 (1)	−19.0 (1)	−20.2 (1)	−18.2 (1)	
log K_3*	−13.16 (2)	−10.89 (10)	−10.24 (4)	−7.94 (4)	−14.3 (1)	20.3 (6)	20.1 (5)	21.4 (4)	18.6 (5)	21.3 (9)	20.5 (16)[j]
log K_1	20.01 (11)[c]	20.07[d]	20.07[d]	17.08 (11)	19.5 (6)	14.9 (5)	14.8 (5)	7.0 (3)	8.6 (4)	7.5 (3)	7.3 (9)
log K_2	14.69 (8)	14.89 (11)	15.12 (8)	13.43 (6)	14.9 (5)	8.8 (5)	9.0 (5)	4.2 (2)	2.9 (3)	5.0 (2)	4.3 (11)
log K_3	9.06 (8)	9.45 (11)	10.10 (6)	9.51 (6)	8.9 (5)	26.64[h]	27.4 (6)[e]	24.1 (5)[f]	23.5 (2)[f]	24.4 (10)[f]	23.5 (7)
other constants								37.0 (6)[g]	36.8 (3)[g]		36.8 (2)
log β_3	43.7 (2)	44.4	45.3	40.0 (1)	43.3 (9)	43.9 (9)	43.9 (9)				
no. of data	112	44	90	73	72	72	161	86	96	99	
GOF	1.1	1.1	2.4	0.8	1.1	1.2	0.9	4.0	1.1	2.2	
(σ_I, σ_Y)[i]	(1.5, 0.1)	(3.0, 1.0)	(3.0, 1.0)	(1.5, 0.3)	(1.0, 0.1)	(1.0, 0.1)	(1.0, 2.0)	(0.5, 0.2)	(0.5, 0.2)	(0.5, 0.2)	

[a] The positions of the substituent groups X, Y, and Z on the catechol ligand are defined by the general species i. [b] Constants[35] determined at 27.1 °C, except in case 4C (19.5 °C). pK_w = 13.93 (27.1 °C), 14.19 (19.5 °C). With the exception of case 5B, solutions were titrated from high pH to low pH. The ferric hydrolysis constants[44] used in this study (and not refined) are −2.56 (log $\beta_{10\bar{1}}$),[35] −2.84 (log $\beta_{20\bar{2}}$), and −6.20 (log $\beta_{10\bar{2}}$). [c] See footnote *d*, Table I. The estimation of errors for log K_n* are discussed in the text. [d] Value used from ref 20, not refined. [e] This is log β_{112}. The species is assumed to involve coordination of the carboxylate group. [f] This is log β_{111}. [g] This is log β_{121} (catechol–salicylate). [h] This is log β_{112} derived from Fe–acetate log K_1.[43] Refinement not successful. [i] See footnote *e*, Table I. [j] These esd's are derived from the dispersion of values in 5A–C about the mean. [k] Log K_n* = log K_n − pK_{a_2} corresponding to $ML_{n-1} + H_2L \rightleftarrows ML_n + 2H^+$. [l] Result number.

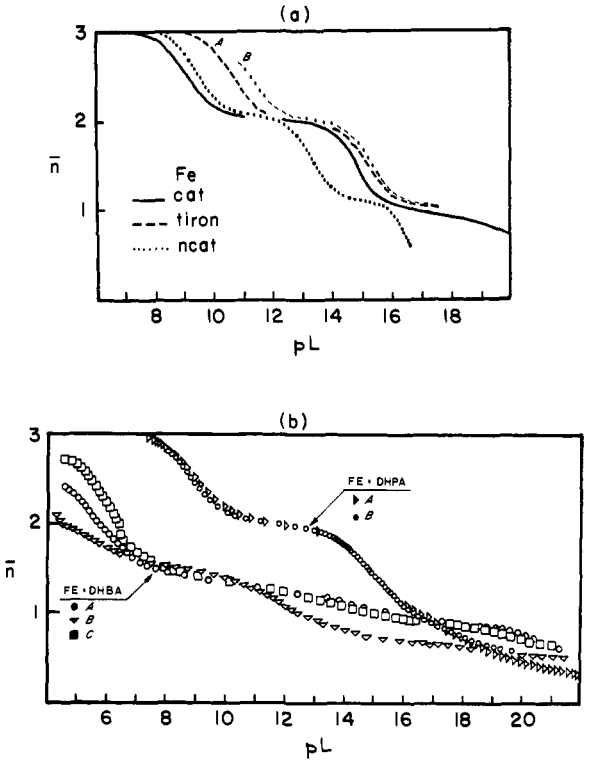

Figure 5. Experimental metal-ligand formation curves (Bjerrum plot). pL = −log [L], where [L] is the concentration of the uncoordinated and fully deprotonated ligand molecule.

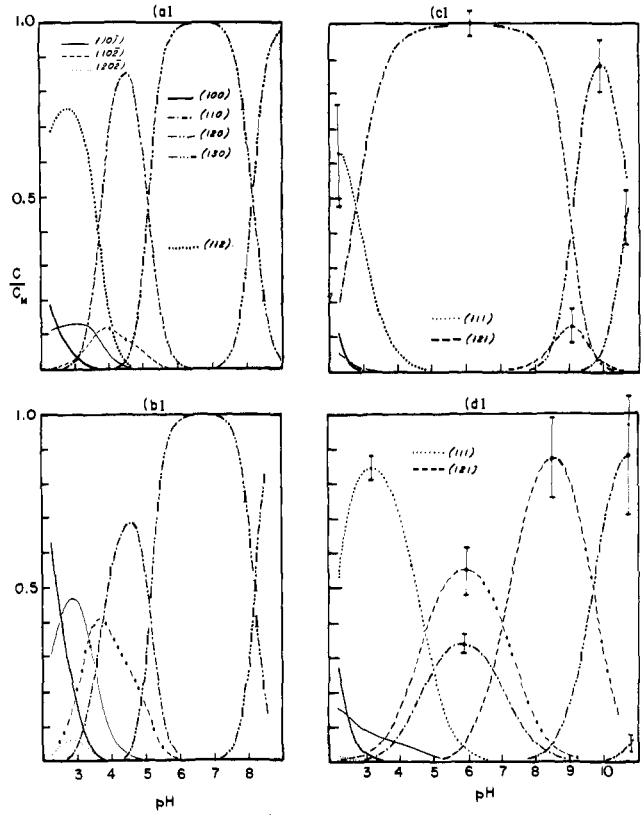

Figure 6. Distribution curves showing relative concentrations of metal-ligand species in solution as a function of pH. For the notation used in describing species, see text. (a) Fe-dhpa, case 4C; (b) Fe-dhpa, case 4A; (c) Fe-dhba, case 5A; (d) Fe-dhba, case 5B. The species are identified by three digits representing the stoichiometric coefficients of the associated complex, in the order metal, ligand, and hydrogen (hydroxide when overlined).

portion of the ligand may be in competition with the catechol portion. The data with $C_L/C_M \sim 13$ were evaluated both with a simple binary model which included only catechol coordination, **6** (case 4A in Table II), and one which also included

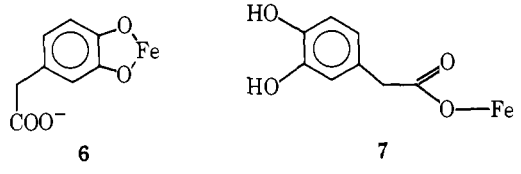

6 **7**

acetate coordination, **7** (4B, Table II). Refinement of the ferric acetate constant (chosen from the literature value for simple ferric acetate complexes[43]) was unsuccessful in the 4B case. It was nevertheless included as a fixed parameter in order to assess its contribution. However, with the C_L/C_M ratio ~6 (case 4C, Table II), variation of the acetate coordination constant was successful. In acidic solutions the resultant differences between the distribution of species predicted by the two models are large. Unlike the other ligand systems (cat, Tiron and ncat), the 4A model for Fe-dhpa showed unusually high correlation[34] (−69%) between log K_1 and log K_2. This high correlation disappeared with the introduction of acetate coordination into the model (cases 4B and 4C).

Ferric-Dihydroxybenzoic Acid. These results are the most difficult to interpret. Comparison of the formation curves of this system with the other ligand systems suggested that a binary model (just catechol coordination) was inadequate, as previously suggested.[14] Because of the complexity of the system, titrations were conducted both from high to low pH (5A, C in Table II) and from low to high pH (case 5B), over a wide range of reagent concentrations. The titration curves (Figure 4) for cases A and C lack one of the inflection points found in case B. The hysteresis between curves 5A and 5B implies that one or both titrations were not at equilibrium. The formation curve for 5B appears to have narrow plateaus at $\bar{n} = 2/3$ and $5/3$ (Figure 5) which occur in pH ranges corresponding to the two inflection points observed in the titration curve. This may be due to salicylate and mixed-mode coordination, shown by **8** and **9.**

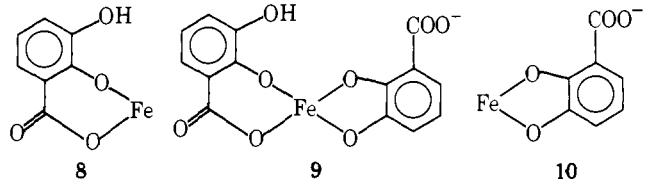

8 **9** **10**

The two high to low pH formation curves (5A and 5C) overlap well for $\bar{n} < 2$. The sharp drop in $\bar{n}$ at pL 6.7 occurred when the experiment was discontinued for about 2 h, suggesting nonequilibrium conditions involving slow rates of reaction. Unlike case 5B, cases 5A and 5C are consistent with the formation of species **9** and **10.** It was possible to refine a model incorporating log β_{111}[35] (salicylate, **8**) and log β_{121} (mixed, **9**) constants in addition to the three binary catechol coordination constants. The distribution curves [Figure 6c for cases 5A,C and Figure 6d for case B] show the bias toward catechol retention when starting the titration from basic solutions and a salicylate bias otherwise. The redistribution of these modes of coordination appears to be slow in basic solutions—the rates of dissociation for such robust complexes are often slow. Another possibility, which was not pursued, is that dimeric species may form under low pH conditions.

Error Analysis. The values of σ_I and σ_V (Tables I and II) reflect the root mean square deviations between the observed and calculated values of pH. Although the estimated standard deviations (esd's) derived from the least-squares refinement

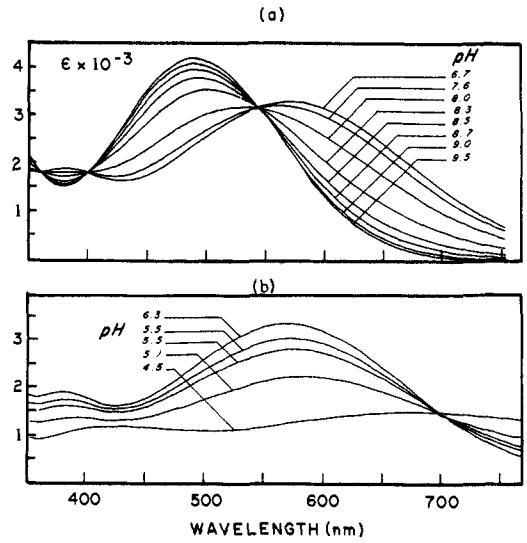

Figure 8. Absorption spectra of aqueous ferric catechol solutions as a function of pH.

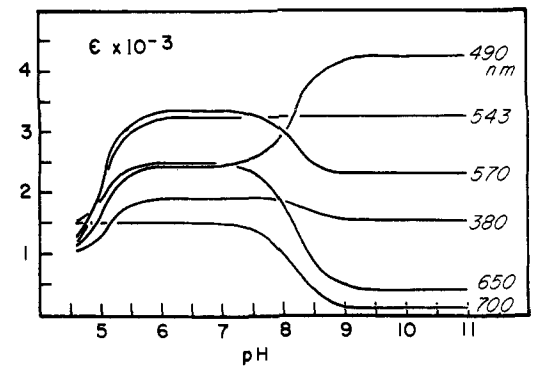

Figure 9. Plots of the molar absorptivities of the ferric catechol system at several wavelengths as a function of pH.

are quite low in the case of the ligand only data (from 0.002 to 0.05 in log units), repeated titrations suggest that these primarily represent random errors (more a measure of precision than accuracy) and that serious systematic errors are difficult to detect from any single titration. This is particularly true in the ferric-dhba titrations (see the esd's of the weighted average values of the several experiments shown in Table II). Even though the least-squares calculated esd's for the pK_as typically are much less than 0.01 for the ligand-only data, a more reasonable estimate of the esd's should be 0.02–0.05 for pK_{a_1} values and 0.1–0.2 for pK_{a_2}, owing to uncertainties in activity coefficients, junction potentials (as a result of uncontrolled ionic strength), buffer pH values, and other systematic errors. In other words, the esd's from the least-squares refinements are measures of the precision of the equilibrium constants. Our experience with repeated measurements under a variety of conditions in other metal–ligand systems suggests that when NBS buffers are used to standardize electrodes, the esd's should be multiplied by the following factors to obtain esd's for the accuracy of the equilibrium constants in regions of pH most sensitive to the determination of the constants:

pH 2–9	$\sigma = 2\sigma_{LS}$ (but in any case ≥ 0.01)
pH 9–11	$\sigma = 3\sigma_{LS}$ (≥ 0.02)
pH >11	$\sigma = 10\sigma_{LS}$ (≥ 0.05)

The accuracy limits quoted for equilibrium reactions of the type

$$ML_{n-1} + H_2L \rightleftharpoons 2H^+ + ML_n \quad (L = \text{catechol dianion})$$

were determined from the the least-squares esd's using the above factors. The standard deviations for the derived formation constants of the type

$$ML_{n-1} + L \rightleftharpoons ML_n \quad (L = \text{catechol dianion})$$

are then determined by summing the variance of the pK_as and the formation constant. These values are all presented in Table II.

The distribution of errors for a single experiment (case 5B) which gave a good fit between data and model are shown in Figure 7.[42b] The nonlinearity of the normal probability curve and the nonuniformity of the error distribution as a function of pH suggest the presence of systematic effects not properly represented in the model. The extent to which seemingly small esd's are propagated to the species distribution curves, as shown by the error bars in Figure 6, was surprising. Speculation regarding the presence of spurious species is easily quelled by the appearance of large errors in such a plot.

Spectroscopic Data. Spectra of catechol–ferric ion solutions were recorded from pH 4.5 to 11 (Figure 8). Below pH 4 the absorption spectrum of the solutions slowly changed with time. For solutions of pH greater than 6, isosbestic points were observed at 400 and at 543 nm. From pH 4.5 to 6.3 only one isosbestic point was observed, at 700 nm. At pH greater than 9.5 the spectra exhibit a maximum at 490 nm (ϵ 4190 L cm^{-1} mol^{-1}). Between pH 6 and 7 the absorption maximum occurs at 570 nm (ϵ 3330 L cm^{-1} mol^{-1}).

Plotting the molar absorptivity vs. pH (Figure 9) reveals two well-separated plateaus indicating that K_2 and K_3 differ by an ample amount. Those wavelengths having the greatest change in absorbance with pH give the more accurate values for K_3. The data were analyzed at 490, 650, and 700 nm.

From Figure 9 it is evident that at pH $\geq$9.5 essentially all of the ferric ion exists as the tris(catecholato) complex while between pH 6 and 7 all of the ferric ion is bound as the bis complex—thereby allowing the determination of ϵ_3 and ϵ_2, the molar absorptivity of the tris and bis complexes, respectively. The value of log K_3 thus obtained (averaged over six pH values at three different wavelengths) is 8.57 (3).

In order to evaluate K_2, the needed value of the molar absorptivity for the 1:1 complex was taken from Mentasti et al.[19a] From their Figure 7 it is possible to estimate ϵ_1^{650nm} 9.0 L cm^{-1} mol^{-1} and ϵ_1^{490nm} 730 L cm^{-1} mol^{-1}. Evaluating the data at 490 and 650 nm gives log K_2 values of 14.9 and 15.2, respectively. The uncertainty of the value of ϵ_1 renders these values only approximate.

The system of ferric ion and dhba is a perplexing one and it was hoped that spectrophotometric titrations would add to the model derived from potentiometric data. Recasting the spectrophotometric data (Figure 10)[42b] in a plot of ϵ vs. pH reveals only one wavelength possibly suitable for the analysis, 615 nm. Indeed such a plot for this sytem lacks horizontal regions suggesting that this system is inappropriate for analysis by the Vareille method. Several possible metal–ligand binding schemes were examined but no agreement with the potentiometric model could be obtained.

In an attempt to determine if the redox reaction between ferric ion and catechol-type ligands was a significant problem in the titrations, the ESR spectra of iron–catechol and iron–Tiron solutions were recorded at different pH. In all cases the spectra exhibited a $g = 4.3$ peak assigned to high-spin ferric ion. In addition, a broad, low-intensity asymmetric signal at $g = 2.3$ of uncertain identity was observed. Finally, in the Tiron system at all pH values from 2.7 through 11.5 no free-radical semiquinone $g = 2.0$ peak was observed except when oxygen was admitted to the tube. For catechol at pH $\geq$5 no semiquinone signal is seen. However, at pH 4.0 a very sharp peak at $g = 2.00$ was observed. In addition, allowing the tube to thaw

at room temperature for about 1 h, then refreezing and recording the spectrum again, results in approximately a 25% decrease in the magnitude of the ferric ion signal. The $g = 4.3$, 2.3, and 2.0 peaks are qualitatively similar to the ESR spectra found in the catechol-binding, non-heme iron-containing enzyme soybean lipoxygenase recently reported by Galpin et al.[46] The reaction is clearly much slower at pH 4.0 than at pH 1-2 as reported by Mentasti et al.[19]

Discussion and Conclusion

By examining the formation constants of ferric complexes with a variety of substituted catechol ligands, we have attempted to establish a reasonable model with which to predict the lower limit for the constants in those ferric siderophore complexes where catechol moieties are the functional units.

The results of the present study and those from reliable past studies delimit the value for the equilibrium constant for the reaction

$$Fe^{3+} + 3\ \text{catechol}^{q-} \rightleftharpoons Fe(\text{catechol})_3^{3-3q}$$

to the range 10^{40}-10^{45}. This number is enormous by comparison to iron complexes with other oxygen-containing ligands. It predicts, for example, that catechol ligands should readily displace cyanide groups from ferricyanide and that Fe_2O_3 (rust) should easily dissolve in basic solutions of catechol. Both reactions occur.

With the exception of the dhba system, which was complicated by mixed-mode coordination, the ligands formed complexes of varying overall stabilities which parallel their ligand base strengths. For a group of similar ligands the plot of the first dissociation constants of the ligands (pK_{a_1}) against the first formation constants of the corresponding metal-ligand complexes (log K_1) is expected to produce a straight line, as shown by Irving and Rossotti[47] for a wide variety of species. Such a plot for ferric catechol complexes (Figure 11) shows linear behavior with sulfonated catechols giving the greatest deviation, to form complexes more stable than predicted. In general there is good correlation between proton and ferric ion affinity with neither steric factors nor the overall charge on the deprotonated ligand contributing greatly to the stability trends.

The ease with which the catechol ligand can reduce ferric ions in acidic solutions depends also on the base strength, since this is a function of both the oxidation potential of the catechol and its ferric ion affinity. The more basic catechols tend to form complexes only at higher pH, since ferric ions must compete with protons for the ligands. Without catechol coordination to provide a strong ligand field, the ferric/ferrous redox potential remains high, near its hexaaquo value (in 1 M acid) of 0.8 V. In the case of coordination by oxalate ligands at pH 5, where a tris complex forms, the potential drops to zero.[48] The qualitative ESR observations in the present study seem to suggest that the ferric state is completely stabilized against reduction by the catechol only with the formation of at least the bis complex. The monocoordinated ferric ion is in equilibrium with the ferrous ion and quinone products, as has been extensively studied in acidic solutions.[19,20] By examining the titration data at higher values of pH in the region of the 1:1 species formation, it was possible to obtain reliable values of log K_1. For example, the value for the constant obtained from kinetic data by Mentasti et al.[19] for the Fe-cat system, 20.9, compares well with ours.

Since the more acidic catechols begin to coordinate ferric ions at lower values of pH, their stability to ferric ion oxidation extends to lower values of pH. This may make such ligands useful as "auxiliary" species in the study of ferric siderophore formation constants: (1) Immobilizing the ferric ions with the weaker catechol species as the metal dissociates from the siderophore may prevent oxidation of the biological ligand. (2)

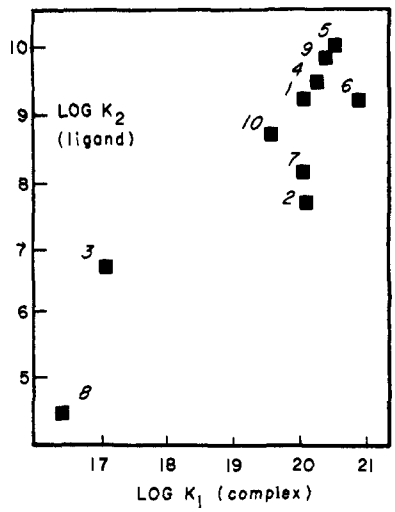

Figure 11. Plot of pK_{a_1} (ligand) vs. log K_1 (complex). Ferric complexes with ligands cat (**1**); Tiron (**2**), ref 13; ncat (**3**); dhpa (**4**); dhba (**5**); cat (**6**), ref 13; 2,3-dihydroxy-6-sulfononaphthalene (**7**), ref 12b; 4-nitroso-5,6-dihydroxybenzene-1,3-disulfonate (**8**), ref 12k; L-3,4-dihydroxyphenylalanine (**9**), ref 13c; 3,4-dihydroxybenzoic acid (**10**), ref 13c.

The auxiliary ligand, being a strong chelator itself, may compete for the metal with the biological counterpart so as to provide an indirect estimate of the siderophore formation constant while not requiring knowledge of the proton dissociation constants of the latter.[49] Such applications are currently being pursued.

When dhba is incorporated into a macrocycle via amide linkages, its basicity would place it in the upper right of Figure 11. Since enterobactin contains three subunits of dhba, the correlation of pK_as and log K_1 values in Figure 11 may be used to estimate a *minimum* value for the formation constant of the ferric enterobactin complex of approximately 10^{45}. Any chelate effect from the entropy advantage of having all three chelating groups part of the same macrocyclic ligand will tend to make the actual formation constant larger than this. Titration data for ferric enterobactin itself are consistent with this prediction.

Acknowledgments. Contributions to the beginning of this research by Mr. J. Hunter Nibert and assistance in the ESR measurements by Dr. Larry Vickery are acknowledged with thanks. Stimulating discussions with Dr. W. P. Schaefer are appreciated. This research is supported by NIH Grant AI 11744. Those parts of the research involving A.A. are supported by the Division of Nuclear Sciences, Office of Basic Energy Sciences, U.S. Department of Energy.

Supplementary Material Available: Figures 2, 7, and 10 (3 pages). Ordering information is given on any current masthead page.

References and Notes

(1) Part 8: K. Abu-Dari and K. N. Raymond, *J. Am. Chem. Soc.*, **99**, 2003 (1977).
(2) (a) J. B. Neilands, Ed., "Microbial Iron Metabolism", Academic Press, New York, N.Y., 1974; (b) J. B. Neilands in "Inorganic Biochemistry", G. Eichhorn, Ed., American Elsevier, New York, N.Y., 1973, p 167 ff; (c) K. N. Raymond, *Adv. Chem. Ser.*, **No. 162** (1977).
(3) (a) J. R. Pollack and J. B. Neilands, *Biochem. Biophys. Res. Commun.*, **38**, 989 (1970); (b) I. G. O'Brien and F. Gibson, *Biochim. Biophys. Acta*, **215**, 393 (1970).
(4) (a) L. Stryer, "Biochemistry", W. H. Freeman, San Francisco, Calif., 1975, pp 796-797; (b) R. Fried, *J. Chem. Educ.*, **45**, 322 (1968).
(5) G. C. Cotzias, M. H. Van Woert, and L. M. Schiffer, *N. Engl. J. Med.*, **276**, 374 (1967).
(6) J. Fermaglich and T. N. Chase, *Lancet*, **1**, 1261 (1973).
(7) B. A. Stoll, *Lancet*, **1**, 431 (1972).
(8) A. C. Andrews, T. D. Lyons, and T. D. O'Brien, *J. Chem. Soc.*, 1776 (1962).
(9) S. Green, A. Mazur, and E. Shorr, *J. Biol. Chem.*, **220**, 237 (1956).
(10) A. Shilov, "Biological Aspects of Inorganic Chemistry" (symposium), University of British Columbia, Vancouver, B.C., June 1976.

(11) G. Vogler, *Arch. Exp. Pathol. Pharmakol.*, **194**, 281 (1940).
(12) (a) A. Willi and G. Schwarzenbach, *Helv. Chim. Acta*, **34**, 528 (1951); (b) G. Heller and G. Schwarzenbach, *ibid.*, **35**, 812 (1952); (c) L. Vareille, *Bull. Soc. Chim. Fr.*, 1496 (1955); (d) R. Nasanen and J. Veivo, *Suom. Kemistil.*, **29B**, 213 (1956).
(13) W. A. E. McBryde, *Can. J. Chem.*, **42**, 1917 (1964).
(14) J. Tsin-Jao, L. Sommer, and A. Okac, *Collect. Czech. Chem. Commun.*, **27**, 1171 (1962).
(15) Y. Murakami and K. Nakamura, *Bull. Chem. Soc. Jpn.*, **36**, 1408 (1963).
(16) M. Beran and S. Havelka, *Collect. Czech. Chem. Commun.*, **32**, 2944 (1967).
(17) R. Abu-Eittah, Z. Mobarak, and S. El-Lathy, *J. Prakt. Chem.*, **316**, 235 (1974).
(18) J. H. Nibert, M. S. Dissertation, University of California, Berkeley, 1975.
(19) (a) E. Mentasti and E. Pelizzetti, *J. Chem. Soc., Dalton Trans.*, 2605 (1973); (b) E. Mentasti, E. Pelizzetti, and G. Saini, *ibid.*, 2609 (1973).
(20) E. Mentasti, E. Pelizzetti, and G. Saini, *J. Inorg. Nucl. Chem.*, **38**, 785 (1976).
(21) (a) S. S. Isied, G. Kuo, and K. N. Raymond, *J. Am. Chem. Soc.*, **98**, 1763 (1976); (b) K. N. Raymond, S. S. Isied, L. D. Brown, F. R. Fronczek, and J. H. Nibert, *ibid.*, **98**, 1767 (1976).
(22) D. A. Scoog and D. M. West, "Fundamentals of Analytical Chemistry", 2nd ed, Holt, Rinehart and Winston, New York, N.Y., 1969, p 690.
(23) L. Meites, Ed., "Handbook of Analytical Chemistry", McGraw-Hill, New York, N.Y., 1963, p 1-20.
(24) G. Gran, *Analyst*, **77**, 661 (1952).
(25) R. G. Bates, "Determination of pH", Wiley, New York, N.Y., 1964.
(26) W. F. Koch, D. L. Briggs, and H. Diehl, *Talanta*, **22**, 637 (1975).
(27) (a) G. E. Mont and A. E. Martell, *J. Am. Chem. Soc.*, **88**, 1387 (1966); (b) C. A. Tyson and A. E. Martell, *ibid.*, **90**, 3379 (1968).
(28) A. Avdeef, to be submitted for publication.
(29) I. G. Sayce, *Talanta*, **15**, 1397 (1968).
(30) A. Sabatini, A. Vacca, and P. Gans, *Talanta*, **21**, 53 (1974).
(31) (a) A. Vacca, A. Sabatini, and M. A. Gristina, *Coord. Chem. Rev.*, **8**, 45 (1972); (b) A. Sabatini and A. Vacca, *J. Chem. Soc., Dalton Trans.*, 1693 (1972); (c) P. Gans and A. Vacca, *Talanta*, **21**, 45 (1974); (d) P. Gans, A. Sabatini, and A. Vacca, *Inorg. Chim. Acta*, **18**, 237 (1976).
(32) For a discussion of weighting schemes in potentiometric data refinement, see, for example, (a) W. P. Schaefer, *Inorg. Chem.*, **4**, 642 (1965); (b) R. C. Lansbury, V. E. Price, and A. G. Smeeth, *J. Chem. Soc.*, 1896 (1965).
(33) (a) B. Sarkar and T. P. A. Kruck, *Can. J. Chem.*, **51**, 3541 (1973); (b) W. A. E. McBryde, *ibid.*, **51**, 3572 (1973).
(34) In certain instances the correlations between overall stability constants[35] for a particular binary complex can be so close to unity as to make refinement unsuccessful. The use of stepwise constants[35] in those instances alleviates the problem. However, in those cases (4A-C, 5A-C, Table II) where log β parameters were introduced, several large correlations arose. For example, log K_1 is correlated by more than 90% with log β_{112} (4C) and log β_{111} (5A and 5C). Also in case 5B, log K_1 and log K_2 are correlated by 83%.
(35) Definitions for the equilibrium constants used in the text include (a) stepwise constant, $K_n = [ML_n]/[ML_{n-1}][L]$, representing $ML_{n-1} + L \rightleftarrows ML_n$, (b) cumulative constant, $\beta_n = [ML_n]/[M][L]^n$, representing $M + nL \rightleftarrows ML_n$, and (c) general cumulative constants, $\beta_{rst} = [M_rL_sH_t]/[M]^r[L]^s[H]^t$. If t in the latter expression is negative, then the implied equilibrium is $rM + sL = tH_2O \rightleftarrows M_rL_s(OH)_t + tH$.
(36) R. Maggiore, S. Musumeci, and S. Sammartano, *Talanta*, **23**, 43 (1976).
(37) C. W. Davies, "Ion Association", Butterworths, London, 1962, p 41.
(38) J. Bjerrum, "Metal Ammine Formation in Aqueous Solution", P. Haase and Son, Copenhagen, 1942.
(39) H. M. Irving and H. S. Rossotti, *J. Chem. Soc.*, 2904 (1954).
(40) See, for example, the discussion of model assessment and related error analysis in ref 31a. The goodness of fit is defined as

$$\sqrt{\left(\sum\left(\frac{\Delta}{\sigma}\right)^2\right)/(n_{obsd} - n_{var})}$$

where Δ is the observed deviation between observed and calculated values, σ is the standard deviation of the observation, n_{obsd} is the number of independent observations, and n_{var} is the number of variables optimized in the refinement.
(41) S. C. Abrahams and E. T. Keve, *Acta Crystallogr., Sect. A*, **27**, 157 (1971).
(42) (a) A. Avdeef, G. G. Christoph, and W. P. Schaefer, to be submitted for publication. (b) See paragraph at end of paper regarding supplementary material.
(43) L. Sommer and K. Pliska, *Collect. Czech. Chem. Commun.*, **26**, 2754 (1961).
(44) C. F. Baes, Jr., and R. E. Mesmer, "The Hydrolysis of Cations", Wiley-Interscience, New York, N.Y., 1976, p 235.
(45) R. F. Jameson and W. F. S. Neillie, *J. Inorg. Nucl. Chem.*, **28**, 2667 (1966).
(46) J. R. Galpin, L. G. N. Tielens, G. A. Veldnik, J. F. G. Vliegenthart, and J. Boldingh, *FEBS Lett.*, **69**, 179 (1976).
(47) H. Irving and H. Rossotti, *Acta Chem. Scand.*, **10**, 72 (1956).
(48) M. Deveux, R. Meilleur, and R. L. Benoit, *Can. J. Chem.*, **46**, 1383 (1968).
(49) F. J. C. Rossotti and H. Rossotti, "The Determination of Stability Constants", McGraw-Hill, New York, N.Y., 1961, p 70 ff.
(50) One of the referees questioned our use of glass electrodes for determining pK_{a_2} (>12). The procedure we used to convert pH (meter reading) to "$[H^+]$" had inherent to it the assumptions that in the regions examined (pH 2-12.7) the junction potential is small and constant. Also the asymmetry potential was assumed to change only very slowly. Since the completion of this work, we have examined this more carefully and observe a junction potential on the order of 2 mV. Not having incorporated this, our pH values may be off by as much as 0.03 pH units. Also the work of Hedwig and Powell[51] suggests that the "operational" activitivities can be described for μ 0.04-0.2 M by $-\log \lambda_{H^+} \sim 0.09-0.005\ p[H^+]$, which has its highest disagreement ($\Delta \log \lambda \sim 0.07$) with activities calculated from the Davies expression[37] at high values of pH. This becomes a problem in the determination of pK_{a_2}s when $K_w/10^{-pH}\ \lambda_{KOH}$ becomes important relative to the magnitude of C_H, which is the case at pH 12. To what extent systematic errors are introduced, we cannot accurately predict. It is for this reason that we think that the esd's calculated from least squares ought to be increased tenfold for pK_{a_2} values. The referee also questioned the pK_{a_2} value for dhpa (our value 13.7, literature value[52] 12.0). We note in the text that the appearance of the proton dissociation curves for that ligand (Figure 3) may suggest some difficulty in ascribing much certainty to that value. We must point out, however, that the corresponding literature value is based only on *one data point*, at which $h = 0.9834$. If $\sigma(h) > 0.01$, which is quite possible, then the literature value of 12.0 is highly suspect. It is our judgment that the sort of estimates we make for the "true" errors in the constants do not alter our general conclusions in the study.
(51) G. R. Hedwig and H. K. J. Powell, *Anal. Chem.*, **43**, 1206 (1971).
(52) V. T. Athavale, L. H. Prabhu, and D. G. Vartak, *J. Inorg. Nucl. Chem.*, **28**, 1237 (1966).